EUROPEAN ORGANIZATION FOR NUCLEAR RESEARCH

MEASUREMENT OF COHERENT ELASTIC AND INELASTIC DEUTERON-PROTON SCATTERING AT s = 2800 GeV^2

J.C.M. Armitage, P. Benz[1], G.J. Bobbink, F.C. Erné, P. Kooijman, F.K. Loebinger, A.A. Macbeth, H.E. Montgomery[2], P.G. Murphy, J.J.M. Poorthuis, A. Rudge, J.C. Sens, D. Stork and J. Timmer

CERN, Geneva, Switzerland
Daresbury Laboratory, U.K.
Foundation for Fundamental Research on Matter (FOM), The Netherlands
University of Manchester, U.K.
University of Utrecht, The Netherlands
(CHM Collaboration)

Abstract

Data on coherent elastic and inelastic deuteron-proton scattering are presented. The measurements were made at the CERN ISR with a single arm spectrometer, at s = 2800 GeV^2 and momentum transfer squared (-t) in the range 0.15 to 0.42 GeV^2.

The data are compared with elastic and inelastic diffractive proton-proton scattering data taken with the same apparatus at the same s and t values. The t dependence of the elastic dp → dp differential cross-section is compared to simple predictions based on Glauber theory. The differential cross-sections for pp → pX and dp → dX are also compared for $M_x^2 \to 280$ GeV^2, where M_x denotes the system of mass x recoiling against the measured proton and deuteron.

Submitted to Nuclear Physics B
September 1977

1) Deceased.

2) Now at Rutherford Laboratory, Chilton, Didcot, Oxon OX11 0QX.

Introduction

The storage of a deuteron beam in one of the CERN Intersecting Storage Rings (ISR) during a development run enabled us to study the coherent elastic scattering reaction:

$$dp \rightarrow dp \qquad (1)$$

as well as the coherent inclusive reaction

$$dp \rightarrow dX \qquad (2)$$

at a centre of mass energy ($\sqrt{s}$) of 53.0 GeV.

The final state deuterons from both reactions were detected at angles between 14 and 25 mrad with respect to the incident deuteron direction. This corresponds to a range of $-0.42 \lesssim t \lesssim -0.15$ GeV^2, where t is the square of the four-momentum transfer between the initial and final state deuterons. For both reactions (1) and (2) this is the region in which rescattering processes (i.e. those in which the emerging proton has interacted with both nucleons in the deuteron) are expected to play a significant role. The semi-classical picture of these rescattering processes is given by Glauber theory[1], but divergences from this picture are expected at high energies[2]. It is therefore of interest to explore this t region for reaction (1), something which has not been previously done at high energies.

In the inelastic reaction (2) the presence of a deuteron in the initial and final states enables us to isolate isoscalar (I=0) exchange processes. In terms of Regge theory one can hence obtain a sample of events in which the Pomeron (diffractive) contribution to high-x inelastic scattering is enhanced (x is the Feynman variable $x=2p_L/\sqrt{s}$). Thus a comparison may be made with the corresponding inclusive process for protons

$$pp \rightarrow pX \qquad (3)$$

where both diffractive and non-diffractive mechanisms are present. Such a comparison can shed some light on the validity of the usual analyses performed on reaction (3) at high energies, where the diffractive mechanism is dominant for high-x values. As this group had previously performed measurements of reaction (3) at ISR energies[3)4)] we were able to make a comparison of reactions (2) and (3) at the same s and t values.

Experimental method

The data were taken with a single-arm magnetic spectrometer which is shown schematically in figure 1. This was placed under the circulating deuteron beam downstream of the ISR intersection region (I2). Its principal element was a septum magnet with an aperture of 60 mm (horizontally) by 100 mm (vertically). The magnet had an integrated field of 2.8 Tesla metres. The spectrometer also contained 14 planes of magnetostrictive spark chambers and 4 trigger counters. The whole assembly was movable and the mean particle production angle accepted by the spectrometer could be varied from 15 to 90 mrad. The momentum resolution of the spectrometer for 26 GeV particles was $\Delta p/p \simeq 2.3\%$ (FWHM). The spectrometer particle track, once analysed, could be projected to intersect the horizontal plane of the deuteron beam and the radial position of the interaction point determined to ± 1 mm. Using the known ISR momentum compaction the momentum of the incident deuteron could thus be determined to ± 0.2%. The particle production angle could be measured with a precision of about ± 0.7 mrad at 26 GeV, i.e. $\Delta t/t$ ± 22% (FWHM) at 15 mrad, decreasing to 13% (FWHM) at 25 mrad.

The intersection region was surrounded by 186 scintillation counters which covered 95% of the full solid angle. The counters were arranged in a central 'barrel' of scintillators (see Ref.(5)) and several 'forward' hodoscopes (H). These counters allowed the charged particle multiplicity associated with a spectrometer event to be measured. One of the H hodoscopes (H14) covered the angular region directly opposite the spectrometer. This hodoscope consisted of 12 narrow scintillators (4.8 cm vertical height) which gave fine

angular binning ($\Delta\theta \sim 12$ mrad)and was used in the identification of elastic events as described below.

The deuteron-proton data presented correspond to an integrated luminosity ($\int Ldt$) of about 470 μb^{-1}, the proton-proton data are a subsample of data on $pp \rightarrow pX$ at $s = 2800$ GeV^2 taken as part of a study of small angle diffractive scattering. For all data the luminosity of the interaction region was continuously monitored by two independent systems, each consisting of two telescopes of three scintillation counters. The telescopes were placed as shown in figure 1. This configuration avoided elastic events which would otherwise have caused excessive sensitivity to the source position. These scintillation counters were large (10 cm high by 50 cm wide) compared to the ISR beam size (about 0.3 x 4 cm) and hence small vertical and radial shifts between different runs at the same ISR energy had a negligible effect on the counting rates. The proportionality constant σ_M which related the luminosity L to the monitor counting rate (dN_M/dt) via

$$\frac{dN_M}{dt} = \sigma_M L \qquad (4)$$

was measured using the Van der Meer method[6] for both pp and dp beams.

The momentum spectrum of detected particles from dp interactions is shown in figure 2a) for a subsample of the data. Events originating outside the intersection region (primarily beam gas scatters which were typically 3-4% of the data) have been removed from the distribution. The spectrum is integrated over the angular range of the spectrometer and is not corrected for its momentum acceptance. Two clear peaks can be seen; one centred at the momentum of the primary beam due to coherently scattered deuterons; the second centred around half the primary beam momentum. The second peak consists of protons from scattering processes in which the deuteron has broken up. The detected proton is either a spectator from a proton-neutron scattering event or a product of a proton-proton scattering event. These two processes can

be written as:

$$n(p_s) + p \rightarrow (p_{s,d}) + X \tag{5}$$

$$p(n_s) + p \rightarrow p_d + (n_s) + X \tag{6}$$

where the subscripts s and d refer to the spectator and detected particles respectively.

Elastic scattering events were identified using the H14 hodoscope. An elastic event was defined as one with one particle detected in H14 within a vertical angular bite of ± 12 mrad with respect to the elastic recoil vector of the spectrometer particle, and no other detected particle. The result of applying this criterion to events in figure 2a) is shown in figure 2b) where a clear coherent elastic deuteron peak stands out. Low recoil-mass inelastic events also peak in the elastic region but much more gently. The H14 counter distributions were examined to find the small fraction of inelastic events contained in the elastic peak and corrections were made for this. Elastic events can be lost from the sample by accidental counts in the hodoscopes and to determine the correction for this effect the H14 counter distributions were again examined for cases with one or two hodoscope counts and a near-elastic recoil. The combined corrections were typically of the order of 5% of the total number of elastic events.

The spectrometer contained no device capable of identifying the detected particle. For pp events this was known to be unnecessary; all positive high momentum particles ($x \gtrsim 0.9$) from these reactions can be assumed to be protons, the measured[3] pion and kaon contamination being less than 1 in 10^3 . A recoil proton from a break-up reaction involving deuterons can occur with a momentum in the deuteron region due to the effect of the Lorentz boost on the Fermi motion of the target nucleons. The transverse component of this Fermi momentum enables spectator protons to leave the ISR vacuum chamber and to be detected in the spectrometer. It is therefore essential to estimate the

contamination of the break up protons as a function of x in the deuteron region ($x > 0.85$).

In the framework of the spectator picture, the shape of the spectator proton spectrum was calculated for reaction (5) by the Monte Carlo method. The Fermi momentum distribution was obtained from the Hamada-Johnston[7] wave function in the parametrisation of McGee[8] and the detected proton was restricted to be produced within the angular range of the spectrometer. Events with a detected spectator proton are expected to dominate the high momentum side of the inelastic break-up proton spectrum as in all other events the proton emerges with less than its original boosted Fermi momentum. We have therefore normalised our generated detected spectator distribution to the measured inelastic spectrum at a momentum of 15 GeV. The result is shown in figure 2c). The generated distribution follows the shape of the measured distribution up to about 20 GeV ($x \simeq 0.75$). It then falls below the measured spectrum as coherent deuteron events come in. Below 15 GeV the measured spectrum rises due to inelastic diffractive events from reaction (6).

Using this model the estimated proton contamination between x of 0.8 and 0.9 is of order 25%, whilst above 0.9 it is entirely negligible.

The possibility exists that the spectator proton momentum distribution is distorted by final state interactions, leading to an enhanced spectator momentum tail. We therefore quote only cross-sections with deuteron $x > 0.9$ to minimise this possible bias.

Results and discussions

a) Elastic scattering

The dp differential elastic cross-sections ($d\sigma/dt$) measured by this experiment are shown in figure 3a) and given in Table I. No data exist on this reaction at ISR energies and the nearest comparison which can be made is with the FNAL data of Akimov et al[9] at $s = 1441$ GeV^2. These data exist for $-t < 0.14$ GeV^2 and are shown as the open

circles in figure 3a). It can be seen that both sets of data match up quite well with one another, thus indicating an absence of strong s dependence at these high energies. Also plotted on figure 3a) are the data on pd elastic scattering from Bradamante et al.[10] at s = 41 and 52 GeV^2. Comparison with our data shows a shrinkage in the shape of $d\sigma/dt$ at these t values, but one which is only very gentle over a large range in s.

The differential cross-section values for pp elastic scattering at s = 2800 GeV^2 obtained from this experiment are shown in figure 3b) and Table I. This reaction has been well measured at ISR energies and hence comparison of our measurements with those of other groups acts as a calibration of the whole procedure of elastic subtraction outlined above. The line on figure 3b) corresponds to the elastic pp data of Barbiellini et al.[11] normalised using the Coulomb-scattering data of Amaldi et al.[12]. Our data agree well with this parametrisation and we are confident that our elastic subtraction has an overall normalisation uncertainty of order 5% which is typically the order of disagreement between different measurements of this reaction.

In order to test the predictions of Glauber theory on our data we have defined the ratio $R_{el}(t)$ as:

$$R_{el}(t) = \frac{d\sigma/dt\big|_{dp \to dp}}{d\sigma/dt\big|_{pp \to pp}} \qquad (7)$$

and our measurements of this ratio are shown in figure 4a). To make predictions for $R_{el}(t)$ we have made some simplifying assumptions about the scattering amplitudes of protons on the individual nucleons in the deuteron. These are:

i) isospin-effects are neglected i.e. the proton-proton and proton neutron amplitudes are assumed equal.

ii) Spin effects in the nucleon-nucleon amplitudes are neglected and the amplitudes are assumed to be entirely spin non-flip . This should be a good approximation at high energies and small angles.

Although the deuteron wave function has a 93% probability of being an S-wave, analyses of coherent reactions at lower energies[13),14)] have concluded that account must also be taken of the D-wave component. The deuteron has unit spin and for unpolarised deuterons the differential cross-section for proton-deuteron scattering must be summed and averaged over final and initial magnetic substates of the nucleus. Therefore the differential cross-section may be written as:

$$\frac{d\sigma}{dq^2} = \frac{\pi}{k^2} \cdot \frac{1}{3} \sum_{M,M'} |F_{M,M'}(\vec{q})|^2 \tag{8}$$

where $\vec{q}$ = three momentum transfer between the initial and final state protons. ($q^2 = -t$).

The Glauber multiple-scattering theory[15)] gives the following form for the amplitudes $F_{M,M'}(\vec{q})$:

$$F_{M,M'}(\vec{q}) = \int d^3r \psi^+_{M'}(\vec{r}) F(\vec{q},\vec{r}) \psi_M(\vec{r}) \tag{9}$$

where $F(\vec{q},\vec{r})$ can be given in terms of the nucleon-nucleon scattering amplitude $f(\vec{q})$ viz:

$$F(\vec{q},\vec{r}) = 2f(\vec{q})\exp(-\tfrac{1}{2}i\vec{q}.\vec{r}) + \frac{i}{2\pi k} \int d^2\vec{q}'\, f(\tfrac{1}{2}\vec{q}+\vec{q}') f(\tfrac{1}{2}\vec{q}-\vec{q}') \exp(-i\vec{q}'.\vec{r}) \tag{10}$$

The deuteron wave function $\psi_M(r)$ can be written as:

$$\psi_M(\vec{r}) = \frac{1}{(4\pi)^{\frac{1}{2}} r} \left[u(r) + \frac{1}{8^{\frac{1}{2}}} S_{12}(\hat{r}) \omega(r) \right] \chi_{1,M} \tag{11}$$

where $u(r)$ and $\omega(r)$ are the S and D wave radial functions; $\chi_{1,M}$ is a spin one spinor, and $S_{12}(\hat{r})$ is the standard tensor operator given by:

$$S_{12}(\hat{r}) = 3(\vec{\sigma}_1.\hat{r})(\vec{\sigma}_2.\hat{r}) - \vec{\sigma}_1.\vec{\sigma}_2 \tag{12}$$

Using equations (8)-(12) Harrington[13] gives the differential cross-section for pd scattering as:

$$\left.\frac{d\sigma}{dt}\right|_{pd \to pd} = \frac{\pi}{k^2}\left[|F_S(\vec{q})|^2 + |F_Q(\vec{q})^2|\right] \tag{13}$$

where

$$F_S(\vec{q}) = 2f(\vec{q})S_s(\tfrac{1}{2}\vec{q}) + \frac{i}{2\pi k}\int d^2\vec{q}'\, f(\tfrac{1}{2}\vec{q}+\vec{q}')f(\tfrac{1}{2}\vec{q}-\vec{q}')S_s(\vec{q}') \tag{14}$$

and

$$|F_Q(\vec{q})|^2 = \frac{3}{4}\left|2f(\vec{q})S_Q(\tfrac{1}{2}\vec{q})\right|^2$$

$$+\frac{1}{4}\left|2f(\vec{q})S_Q(\tfrac{1}{2}\vec{q}) + \frac{i}{2\pi k}\int d^2\vec{q}'\, f(\tfrac{1}{2}\vec{q}+\vec{q}')f(\tfrac{1}{2}\vec{q}-\vec{q}')S_Q(\vec{q}')\right|^2 \tag{15}$$

The functions S_s and S_Q are the deuteron's SPHERICAL and QUADRUPOLE form factors. They are given by the following integral expressions:

$$S_s(q) = \int_0^\infty dr\, \left[u^2(r) + \omega^2(r)\right] j_0(qr) \tag{16}$$

$$S_Q(q) = \int_0^\infty dr\, 2\omega(r)\left[u(r) - \frac{1}{\sqrt{8}}\omega(r)\right] j_2(qr) \tag{17}$$

Equations (13)-(17) can be used to calculate $d\sigma/dt$ for proton-deuteron scattering and hence $R_{el}(t)$ through the relationship

$$R_{el}(t) = \frac{|F_s(\vec{q},s')|^2 + |F_Q(q,s')|^2}{|f(q,s)|^2} \tag{18}$$

where s' is the centre of mass energy squared of an incident proton and a target (deuteron) nucleon and s is the centre of mass energy squared of the colliding pp system. Note that s' varies due to the Fermi

momentum of the nucleons in the deuteron but as the amplitudes for pp elastic scattering are known to be only slowly varying functions of s we can assume s' to be fixed. For our case we have $s' \simeq s/2$.

Using McGee's[8] form for $u(r)$ and $\omega(r)$ we have calculated the prediction for $R_{el}(t)$ from equation (18). For the nucleon amplitudes we have taken:

i) an imaginary part with a pure exponential q^2 behaviour viz:

$$\text{Im } f(s,q) = \frac{k\sigma_{pp}(s)}{4\pi} \exp(-\tfrac{1}{2}a(s)q^2)$$

where $\sigma_{pp}(s)$ is the total proton-proton cross-section. The values of σ_{pp} and a were taken from parametrisations given by Wetherell[17] and Giacomelli[18] respectively. This form is compatible with published data on pp elastic scattering for $-q^2 < 0.3$ at FNAL and ISR energies.

ii) A real part which follows the derivative relation[19]

$$\text{Re } f(s,q) \approx \frac{\pi \, d(\text{Im } f(s,q))}{2d(\ln s)}$$

Equation (19) is derived by an approximation from dispersion relations and provides a method of estimating the phase of the pp amplitude away from $q^2 = 0$ at high energies.

This model gives the solid line prediction in figure 4a). It can be seen that the prediction offers a fairly good description of the data at the 20-25% level. When considering the agreement of the data with our model it is essential to bear in mind that the theoretical prediction is sensitive at the level of ± 25% to the details of the model. The main sources of this sensitivity are:

i) The parametrisations of the nucleon amplitudes which lead to errors of order 10-15% in $d\sigma/dt$ for pp scattering.

ii) The percentage of D-wave admixture present in the deuteron. The Hamada-Johnston wave function used in our predictions has a D-state

probability of $\sim$ 7%. Other wave functions exist[20] with D-state probabilities as low as $\sim$ 4%, which describe low energy nucleon-nucleon scattering and deuteron photodisintegration equally well. Since the D-wave contribution comes in as an amplitude (and hence the square root of the probability) a rough estimate shows that up to 25% variation may be expected in the prediction from using two different acceptable D-wave probabilities.

With these provisos in mind we can still see that our simple Glauber prediction performs just as well as similar analyses at lower energies[10),15)]. This lack of energy dependence in the deuteron spherical and quadrupole scattering amplitudes is brought out in figure 4b) which shows our measurements of $R_{el}(t)$ compared to those of other groups at lower energies.

The effect of ignoring the D-wave component and essentially using only $F_s(q)$ is also shown by curves on figure 4a). The dashed curve keeps the complex amplitudes as outlined above whilst the dotted curve uses only purely imaginary (diffractive) pp amplitudes. A deep minimum (actually a zero for the dotted curve) is predicted around $-t \simeq 0.32$ GeV^2. This is caused by the destructive interference of the two terms in (14). The second term corresponds to events where the proton has scattered off both nucleons in the deuteron. This double scattering term is negligible at small $|t|$ but is the dominant process for $-t > 0.5$ GeV^2 as is has a much gentler fall off than the first (single scattering) term. Consideration of figure 4a) shows that the D-wave component has an important effect only in the region of the interference minimum in $F_s(\vec{q})$, elsewhere it is negligible.

As indicated in the introduction an effect which is expected to become important at high enough energies is that of coherent rescattering of inelastic states produced after the first scatter in the deuteron. Following Good and Walker[21] we note that for small momentum transfers the change in the longitudinal momentum (Δp_ℓ) needed to produce a mass M^* is:

$$\Delta p_\ell \simeq (M^{*2} - m_p^2)/2p$$

where p is the incident proton momentum. For coherent rescattering to occur the change in the wave number for the incident proton (Δk) has to obey a relationship such that $\Delta k.r_D < 1$, where r_D is the deuteron radius. Thus an inelastic intermediate state with mass M^* will only coherently rescatter if

$$M^{*2} - m_p^2 \lesssim 2p/r_D \qquad (20)$$

Equation (20) shows that the allowable range of M^* increases with increasing s. It has been postulated by Pumplin and Ross[2] that the creation of such M^* states leads to a change in the Glauber prediction since the double scatter amplitudes must include a sum over masses up to some maximum term. The theory of this effect has been dealt with by several authors[22] but is very model dependent and detailed application to our data would not be appropriate. We wish to note however that in view of the reasonable fit obtained using only elastic rescattering and the quadrupole moment it seems likely that inelastic rescattering effects do not play an important role in pd scattering out to t values of around -0.4 GeV^2.

b) Inelastic coherent scattering

The data on the invariant differential cross-section for reaction (2) are shown in figure 5 and Table II for t values from -0.15 to -0.3 GeV^2. The data are given as a function of M_x^2/s (M_x is the mass of the system X recoiling against the deuteron), for $M_x^2/s < 0.1$. The value of M_x^2 is related to the c.m. energy of the observed deuteron (E_d) by:

$$M_x^2 = s + m_d^2 - 2\sqrt{s}\ E_d$$

which for large values of s and $M_x^2 \gg m_d^2$ can be approximated by

$$M_x^2 \simeq s\ (1 - x_d)$$

As noted above for $x > 0.9$, ie $M_x^2/s < 0.1$, the background it thought to be much less than 10% and hence no background subtraction has been attempted on this data.

The experimental resolution in M_x^2/s can be estimated from examination of plots for elastic events. From this method we obtain a resolution of 0.01 (standar deviation) for these data. This means that the mass resolution in this experiment was not adequate to examine the diffractive resonance structure in the region $M_x < 4$ GeV, which is seen in pd data measured by Akimov et al.[25] in the range $180 < s < 1441$ GeV^2.

In common with the relationship between the dp and pp elastic differential cross-section, the invariant inelastic differential cross-section for $dp \to dX$ is lower than that for $pp \to pX$ at the t values measured. It exhibits the same peak towards low values of M_x as seen in the pp case[3]. The FNAL data on $pd \to Xd$[25] showed that at low values of t ($0.03 < |t| < 0.12$ GeV) the differential cross-section followed the relation:

$$\frac{d^2\sigma}{dtdM_x^2}\,(pd \to Xd) = \frac{d^2\sigma}{dtdM_x^2}\,(pp \to Xp)\; R_{el}(t) \qquad (21)$$

where $R_{el}(t)$ is the elastic pd/pp ratio as defined previously. In that range of t values, where single scattering dominates, the ratio for both elastic and inelastic reactions is essentially determined by the value of the form factor at t/4 (see (4)) which enables equation (21) to be used.

For the t values covered by this experiment, where double scattering is important, it is no longer clear that such a simple relationship as equation (21) should hold. Comparison of the diffractive cross-sections in Table II and the corresponding quantities for $pp \to pX$ scaled down by $R_{el}(t)$ as given in Table I indicates that the scaled proton invariant cross-sections are about 20-30% lower than those for $dp \to dX$. Thus equation (21) is not satisfied for our data,

though the magnitude of the divergence from (21) is not large.

One can define the single diffractive (sd) region in $pp \rightarrow pX$ scattering as the region with $M_x^2/s < 0.05$. In this region $\sim 98\%$ of the inclusive differential cross-section is expected to be diffractive and since the cross-section for $dp \rightarrow dX$ is of a diffractive nature we may define the ratio:

$$R_{sd}(t) = \frac{\frac{1}{\pi}\int_{-\infty}^{0.05} \frac{d^2\sigma}{dt dM_x^2/s}\, dM_x^2/s \;\Big|_{dp \rightarrow dX}}{\frac{1}{\pi}\int_{-\infty}^{0.05} \frac{d^2\sigma}{dt dM_x^2/s}\, dM_x^2/s \;\Big|_{pp \rightarrow pX}} \qquad (22)$$

This quantity can be used to scale down the proton data, a process which amounts to checking of relative shapes of the deuteron and proton missing mass distributions in the single diffractive region. Table III shows the values of the integrals and the corresponding values of $R_{sd}(t)$, and all quantities are plotted in figure 6. $R_{sd}(t)$ is somewhat bigger than $R_{el}(t)$ and it shows a similar behaviour, flattening off with increasing momentum transfer. As in elastic scattering, the slope of the inelastic pd-distribution is just over twice that of pp inelastic scattering. In the limited t range covered by this experiment both distributions can be adequately described by simple exponentials. For the $dp \rightarrow dX$ data the slope parameter is about 15.1 GeV^{-2} whilst for $pp \rightarrow pX$ it has a value of around 6.5 GeV^{-2}.

The result of scaling the invariant proton differential cross-sections by $R_{sd}(t)$ is shown in figure 5. It may be seen that the scaled proton distributions agree very well with the deuteron distributions for $M_x/s < 0.05$ and also agree within errors up to $M_x^2/s \simeq 0.1$.

This result implies that $R_{sd}(t,M_x^2)$ is largely independent of M_x^2 (at least to 20%) for $M_x^2/s < 0.05$. Although this is not immediately obvious from the Glauber-type expression for inelastic coherent scattering it can be explained phenomenologically in the following way. At small t values where single scattering processes dominate $R_{sd}(t,M_x^2)$ will be independent of M_x^2 as we can write

$$R_{sd}(t,M_x^2) \simeq \frac{|2f_i(\vec{q},M_x^2)S_{TOT}(\vec{q}/2)|^2}{|f_i(\vec{q},M_x^2)|^2} \qquad (23)$$

where $S_{TOT}(\vec{q})=S_s(\vec{q})+S_Q(\vec{q})$

and $f_i(\vec{q},M_x^2)$ is the amplitude for $pp \to pX$.
Equation (23) is clearly independent of M_x^2. The equivalent double scattering term contains an integration over of all possible intermediate states, but at small t it is predominantly composed of one elastic and one inelastic amplitude and hence leads to a similar cancellation as in (23).

The empirical agreement between the shapes of the M_x^2 distributions for $pp \to pX$ and $dp \to dX$ is still unexpected when viewed in terms of particle exchanges. As noted in the introduction the exchanged particles in $dp \to dX$ are restricted to I=0. Most analyses of the diffractive peak in $pp \to pX$ using the Triple-Regge formalism[26] demand an increasing non-diffractive term for $M_x^2/s > 0.05$. Following the notation of reference (26) this is an (MMP) term (M=Meson, P=Pomeron) and it is found to give a contribution to the invariant differential cross-section equal to the leading diffractive (PPP or triple-Pomeron) term at $M_x^2/s \simeq 0.1$ at $s \simeq 400$ GeV^2. Since both of these terms are s-independent we expect the same situation to apply for our data. Hence the $dp \to dX$ data, where no (MMP) term is possible, should be about 50% of the $pp \to pX$ data at $M_x^2/s \simeq 0.1$ when the two distributions are normalised for $M_x^2/s < 0.05$. The fact that this is not seen by us casts some doubt on the conventional Triple-Regge analyses of this type.

Conclusions

Our conclusions are as follows:

I) The data for dp elastic scattering show a gradually flattening t-dependence between $-0.15 > t > -0.42$ GeV^2. Very little energy dependence is exhibited in the t-distribution between $\sqrt{s} = 38$ and $\sqrt{s} = 53$ GeV^2. A slight shrinkage is detectable in the above t range

between PS and ISR energies.

2) The data on the ratio of the differential elastic cross-sections for dp → dp and pp → pp are quite well fitted using the simple Glauber model with the inclusion of the deuteron quadrupole moment. The inelastic rescattering mechanism does not appear to give an important contribution to the dp elastic cross-section in the t range covered by this experiment.

3) The missing mass distribution for dp → dX has a very similar shape to that for pp → pX for values of $M_x^2/s < 0.1$. The ratio of the two distributions at the same t is equal to $R_{sd}(t)$ where $R_{sd}(t)$ is the ratio of integrals of the invariant differential cross-sections for dp → dX and pp → pX taken up to a value of $M_x^2/s = 0.05$. The similar shape for dp → dX and pp → pX is at variance with the pr predictions of conventional Triple-Regge analyses.

Acknowledgment

We would like to acknowledge the excellent work of the machine physicists in the PS and ISR divisions in making the acceleration and storage of deuterons a reality. We are also grateful to the ISR Experimental Support, Vacuum, Operations and Survey Groups for their assistance. Useful conversations with Dr. A.C. Phillips are also acknowledged. This experiment has been supported by the Nederlandse Organisatie voor Zuiver Wetenschappelijk Onderzoek through F.O.M., and by the U.K. Science Research Council through the Daresbury Laboratory.

We would like to pay a special tribute to our fellow-colleague and friend Peter Benz, who worked with us in the team and who was closely involved with the analysis of this experiment. It was with great sadness that we learned of his death on 13.7.1977.

References

1) See for instance R.J. Glauber in 'Lectures in Theoretical Physics', edited by W.E. Brittin et al. (Interscience Publishers Inc., New York, 1959), Vol. 1, p. 315.

2) J. Pumplin and M. Ross, Phys. Rev. Letts. 21 (1968 1778.

3) M.G. Albrow et al., Nucl. Phys. B108 (1976) 1 and references to earlier CHLM collaboration work contained therein.

4) J.C.M. Armitage et al., to be submitted to Nucl. Phys. B.

5) M.G. Albrow et al., Nucl. Phys. B102 (1976) 275.

6) S. Van der Meer, CERN Internal Report, ISR-PO/68-31 (1968).

7) T. Hamada and I.D. Johnston, Nucl. Phys. 34 (1962) 382.

8) I.J. McGee, Phys. Rev. 151 (1966) 772.

9) Y. Akimov et al., Phys. Rev. D12 (1975) 3399 and references contained therein.

10) F. Bradamante et al., Phys. Letts. 32B (1970) 303.

11) G. Barbiellini et al., Phys. Letts. 39B (1972) 663.

12) U. Amaldi et al., Phys. Letts. 44B (1973) 112.

13) D.R. Harrington, Phys. Rev. Letts. 21 (1968) 1496.

14) V. Franco and R.J. Glauber, Phys. Rev. Letts. 22 (1968) 370.

15) V. Franco and R.J. Glauber, Phys. Rev. 142 (1966) 1195.

16) J.H. Blatt and V.F. Weisskopf, Theoretical Nuclear Physics (John Wiley and Sons, Inc., New York, 1952) p. 100.

17) A.M. Wetherell, rapporteur's talk, EPS Conference on High Energy Physics, (Palermo 1975) ed. A. Zichichi (Editrice Compositori-Bologna).

18) G. Giacomelli, 'Total Cross-Sections and Elastic Scattering at High Energies', Physics Reports 23C (2), (1976) p. 182.

19) See for example J.B. Bronzan, G.L. Kane and U.P. Sukhatme NAL-Pub-74/23-THY (1974) and Phys. Letts. 49B (1974) 272.

20) See for example A.C. Phillips 'Three Body Systems in Nuclear Physics', University of Manchester preprint (1977) p. 26-29 (to be published in Reports on Progress in Physics).

21) M.L. Good and W.D. Walker, Phys. Rev. 120 (1960) 1857.

22) See for example V.V. Anisovich, P.E. Volkovitsky and L.G. Dakhno Phys. Letts. 42B (1972) 244.
C. Quigg and L.L. Wang, Phys. Letts. 43B (1973) 314, and references contained therein.
E.M. Levin et. al., Nucl. Phys. B124 (1977) 539.

23) J.V. Allaby et al., Nucl. Phys. B52 (1973) 316.

24) FNAL Spectrometer Group, Phys. Rev. Letts. 35 (1975) 1195.

25) Y. Akimov et al., Phys. Rev. Letts. 35 (1975) 763.

26) D.P. Roy and R.G. Roberts, Nucl. Phys. B77 (1974) 240.

Figure captions

Fig. 1. Schematic plan and elevation views of the apparatus. The abbreviations used are as follows:
A1, A2 - support arms
B - 'Barrel' of scintillation counters.
H11, H12, H13, H14, H21, H22 - Hodoscopes.
(U1,U2) and (D1,D2) - Luminosity monitor telescopes.
T1 - T4 - Trigger counters.

Fig. 2a) Momentum spectrum of particles detected by the small angle spectrometer.
b) Momentum spectrum of the subsample of events which satisfied the elastic criterion (see text).
c) Momentum spectrum of inelastic events compared to the predicted proton distribution from a simple spectator model (see text).

Fig. 3a) Measurements of the elastic differential cross-section ($d\sigma/dt$) for $dp \to dp$ from this experiment and references (9) and (10).
b) Measurements of ($d\sigma/dt$) for $pp \to pp$ from this experiment.

Fig. 4a) Measurements of $R_{el}(t)$ (see text) from this experiment compared with various predictions based on Glauber scattering theory.
b) Measurements of $R_{el}(t)$ from this experiment ($s = 2813\ GeV^2$) compared to values of $R_{el}(t)$ calculated from other measurements at lower energies. The $s = 48\ GeV^2$ results are calculated from Bradamante et al.[10] and Allaby et al.[23]. The $s = 262\ GeV^2$ results are calculated from Akimov et al.[9] and the FNAL Single Arm Spectrometer Group.

Fig. 5. Invariant differential cross-sections for $dp \to dX$ compared to cross-sections for $pp \to pX$ scaled down by $R_{sd}(t)$ as defined in the text.

Fig. 6. Measurements of the 'single-diffractive' $d\sigma/dt$ (see text) for $pp \to pX$ and $dp \to dX$, and the ratio between the two, R_{sd}, compared with R_{el}.

TABLE I

$-t$ (GeV^2)	$\frac{d\sigma}{dt}$ ($dp \to dp$) (mb/GeV^2)	$\frac{d\sigma}{dt}$ ($pp \to pp$) (mb/GeV^2)	$R_{el}(t) = \frac{d\sigma/dt\,\vert_{dp \to dp}}{d\sigma/dt\,\vert_{pp \to pp}}$
0.13	-	21.1 ± 0.3	-
0.15	2.52 ± 0.11	18.0 ± 0.2	(13.6 ± 0.7) x 10^{-2}
0.17	1.60 ± 0.09	14.5 ± 0.2	11.0 ± 0.6 "
0.19	0.97 ± 0.06	10.6 ± 0.2	9.2 ± 0.6 "
0.21	0.54 ± 0.05	8.02 ± 0.15	6.7 ± 0.6 "
0.23	0.32 ± 0.04	6.25 ± 0.13	5.0 ± 0.6 "
0.26	0.23 ± 0.04	5.05 ± 0.16	4.5 ± 0.7 "
0.30	0.093 ± 0.025	3.09 ± 0.10	3.0 ± 0.8 "
0.34	0.055 ± 0.019	1.85 ± 0.07	3.0 ± 1.0 "
0.38	0.030 ± 0.008	1.12 ± 0.05	2.7 ± 0.8 "
0.42	0.025 ± 0.009	1.03 ± 0.05	2.4 ± 0.9 "
0.46	-	0.69 ± 0.07	-

TABLE II

Invariant differential cross-section $\frac{1}{\pi}\frac{d^2\sigma}{dtd(M_x^2/s)}$ (mb/GeV) for $dp \to dX$.

M_x^2/s	INVARIANT CROSS-SECTION (σ_{inv})						M_x^2/s	σ_{inv}
	t = -0.15	t = -0.17	t = -0.19	t = -0.21	t = -0.23	t = -0.26		t = -0.3
-0.024	0.55 ± 0.41	0.33 ± 0.22	0.29 ± 0.17	0.18 ± 0.11	0.23 ± 0.13	0.20 ± 0.12	-0.013	0.28 ± 0.18
-0.019	1.29 ± 0.51	1.27 ± 0.48	0.77 ± 0.29	0.21 ± 0.10	0.21 ± 0.10	0.52 ± 0.19	-0.008	1.29 ± 0.45
-0.013	3.82 ± 1.03	2.75 ± 0.73	1.82 ± 0.50	1.07 ± 0.27	0.72 ± 0.21	0.6 ± 0.18	-0.003	1.77 ± 0.5
-0.008	6.86 ± 1.44	5.81 ± 1.15	3.74 ± 0.75	2.25 ± 0.41	1.68 ± 0.33	1.74 ± 0.35	0.003	1.05 ± 0.41
-0.003	11.35 ± 1.57	8.31 ± 1.17	5.81 ± 0.83	3.76 ± 0.51	2.47 ± 0.37	2.48 ± 0.39	0.008	1.39 ± 0.49
0.003	13.17 ± 1.97	10.38 ± 1.51	7.85 ± 1.15	4.26 ± 0.58	2.31 ± 0.40	2.48 ± 0.42	0.013	0.69 ± 0.33
0.008	11.13 ± 1.54	8.04 ± 1.1	6.77 ± 0.94	4.72 ± 0.61	2.77 ± 0.47	2.46 ± 0.41	0.019	1.06 ± 0.46
0.013	8.47 ± 1.19	7.41 ± 1.1	4.94 ± 0.80	3.04 ± 0.48	2.08 ± 0.40	1.73 ± 0.35	0.024	0.56 ± 0.46
0.019	5.75 ± 0.81	4.07 ± 0.65	3.94 ± 0.66	1.64 ± 0.33	1.54 ± 0.34	0.89 ± 0.23	0.029	0.37 ± 0.24
0.024	4.21 ± 1.00	3.63 ± 0.84	3.07 ± 0.79	2.06 ± 0.41	1.00±± 0.36	0.61 ± 0.26	0.035	0.61 ± 0.36
0.029	3.84 ± 0.64	3.71 ± 0.63	1.84 ± 0.46	1.58 ± 0.42	1.14 ± 0.33	0.82 ± 0.30	0.043	0.24 ± 0.16
0.035	2.52 ± 0.51	2.54 ± 0.52	1.42 ± 0.38	1.37 ± 0.34	0.88 ± 0.28	0.68 ± 0.20	0.053	0.4 ± 0.2
0.040	3.08 ± 0.56	1.88 ± 0.44	1.78 ± 0.44	0.88 ± 0.31	0.88 ± 0.28	0.34 ± 0.17	0.064	0.27 ± 0.16
0.045	2.77 ± 0.52	2.11 ± 0.47	2.02 ± 0.46	1.09 ± 0.31	0.69 ± 0.29	0.84 ± 0.23		
0.051	2.19 ± 0.45	2.89 ± 0.53	1.64 ± 0.41	0.86 ± 0.27	0.59 ± 0.23	0.65 ± 0.22		
0.056	1.97 ± 0.44	3.14 ± 0.55	1.92 ± 0.45	0.82 ± 0.28	0.78 ± 0.27	0.39 ± 0.14		
0.061	1.88 ± 0.42	2.44 ± 0.49	1.68 ± 0.43	0.98 ± 0.30	1.00 ± 0.30	0.35 ± 0.12		
0.067	2.74 ± 0.51	2.51 ± 0.51	1.69 ± 0.41	1.23 ± 0.34	0.59 ± 0.23	0.66 ± 0.24		
0.075	1.87 ± 0.30	1.75 ± 0.29	1.82 ± 0.30	1.11 ± 0.21	0.88 ± 0.21	0.58 ± 0.13		
0.085	1.66 ± 0.28	1.78 ± 0.29	1.47 ± 0.29	0.60 ± 0.18	0.88 ± 0.19	0.60 ± 0.15		
0.096	1.37 ± 0.25	2.38 ± 0.34	1.38 ± 0.27	0.77 ± 0.20	0.58 ± 0.15	0.41 ± 0.12		

TABLE III

Integrated invariant differential cross-section $\int_{-\infty}^{0.05} \frac{d^2\sigma}{dt\,d(M_x^2/s)}\, d(M_x^2/s) = \sigma_{sd}$

for $pp \to pX$ and $dp \to dX$ and the ratio $R_{sd} = \frac{\sigma_{sd}(dp \to dX)}{\sigma_{sd}(pp \to pX)}$

$-t$ (GeV^2)	σ_{sd} $dp \to dX$ (mb/GeV^2)	σ_{sd} $pp \to pX$ (mb/GeV^2)	$R_{sd}(-t)$
0.15	1.34 ± 0.07	8.11 ± 0.15	(16.5 ± 0.9) x 10^{-2}
0.17	1.07 ± 0.05	7.69 ± 0.15	13.9 ± 0.7 "
0.19	0.79 ± 0.04	6.44 ± 0.16	12.3 ± 0.7 "
0.21	0.48 ± 0.03	5.59 ± 0.13	8.6 ± 0.6 "
0.23	0.32 ± 0.02	4.74 ± 0.12	6.8 ± 0.5 "
0.26	0.29 ± 0.02	4.22 ± 0.15	6.9 ± 0.5 "
0.3	0.17 ± 0.02	3.29 ± 0.10	5.2 ± 0.6 "

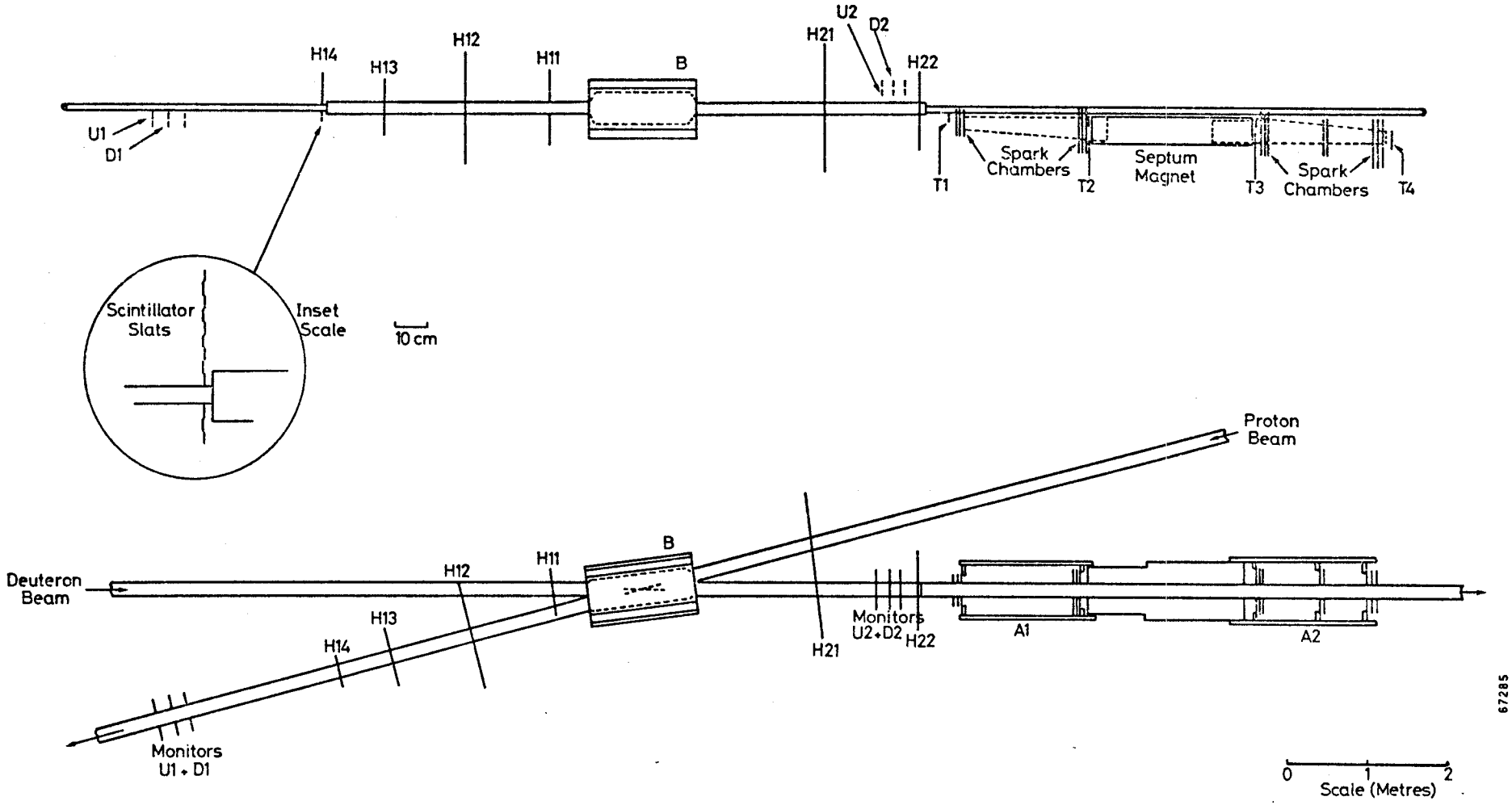
U1
D1
H14
H13
H12
H11
B
H21
U2
D2
H22
T1
Spark Chambers
T2
Septum Magnet
T3
Spark Chambers
T4
Scintillator Slats
Inset Scale
10 cm
Proton Beam
Deuteron Beam
H12
H11
B
H13
H14
H21
Monitors U2+D2
H22
A1
A2
Monitors U1+D1
0
1
2
Scale (Metres)
67285

Fig.1

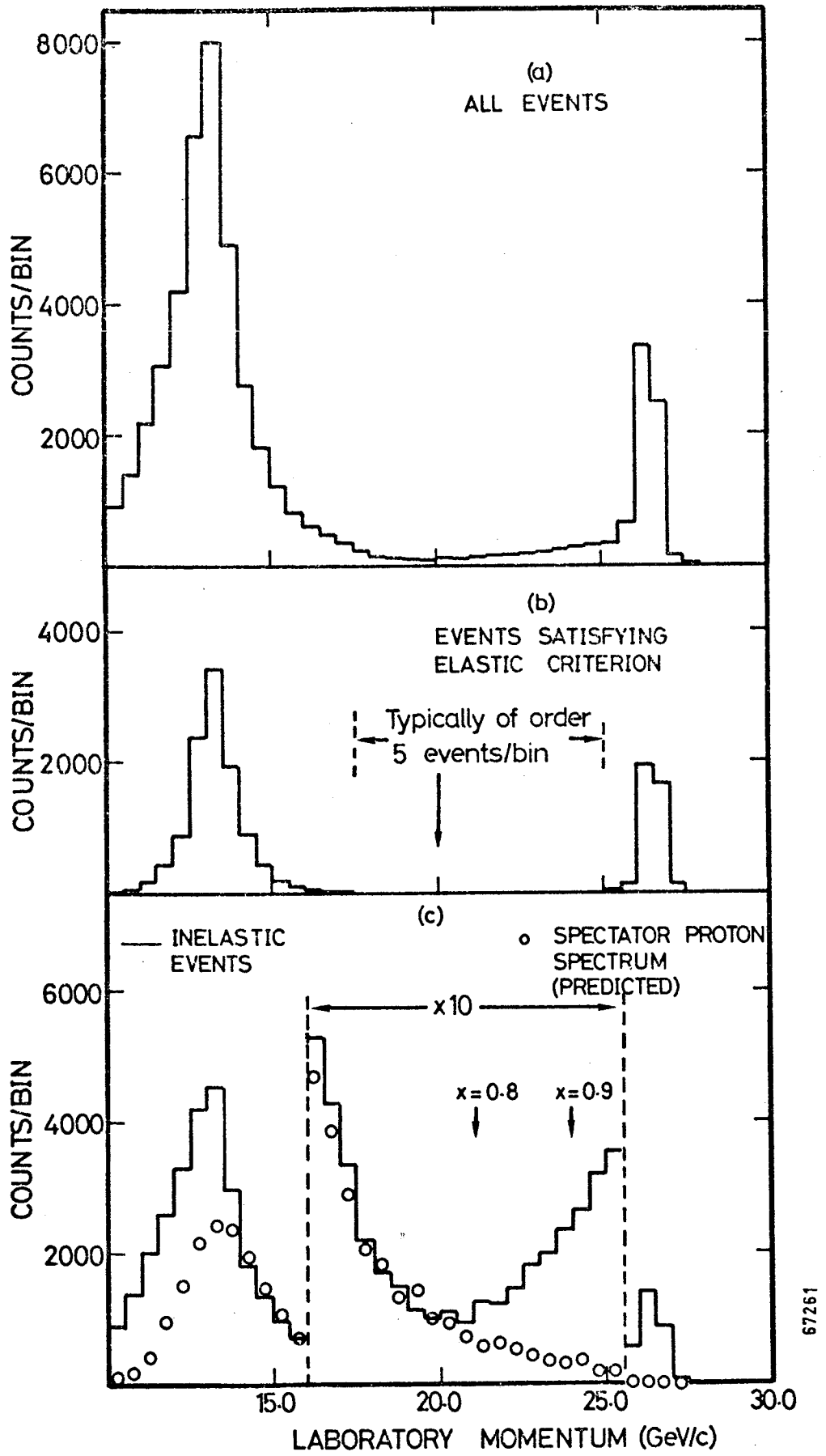
8000
6000
4000
2000
COUNTS/BIN
(a)
ALL EVENTS
4000
2000
COUNTS/BIN
(b)
EVENTS SATISFYING
ELASTIC CRITERION
Typically of order
5 events/bin
(c)
INELASTIC
EVENTS
SPECTATOR PROTON
SPECTRUM
(PREDICTED)
x10
x=0·8
x=0·9
6000
4000
2000
COUNTS/BIN
15·0
20·0
25·0
30·0
LABORATORY MOMENTUM (GeV/c)
67261

Fig.2

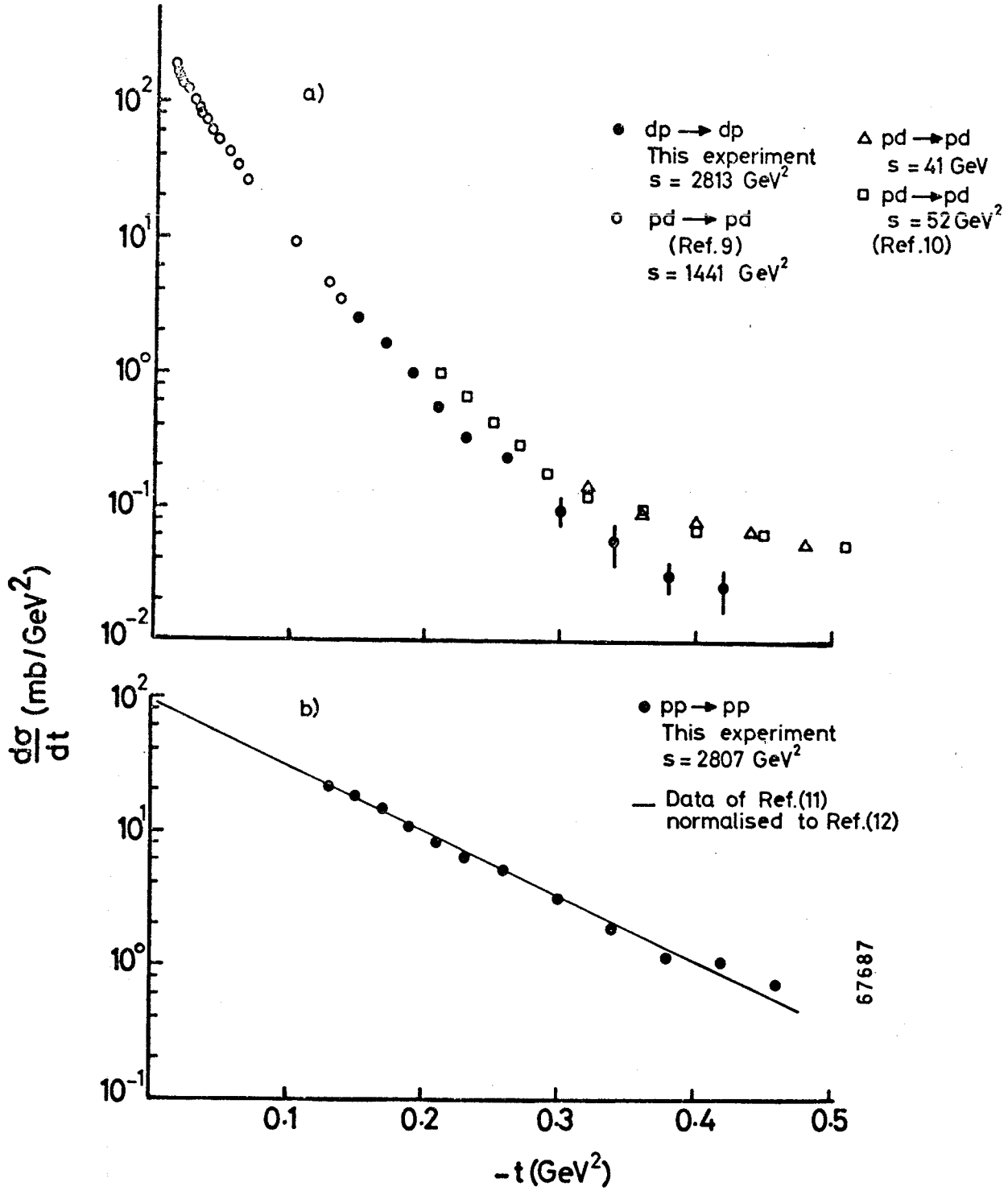
a)
dp → dp
This experiment
s = 2813 GeV²
pd → pd
(Ref. 9)
s = 1441 GeV²
pd → pd
s = 41 GeV
pd → pd
s = 52 GeV²
(Ref. 10)
b)
pp → pp
This experiment
s = 2807 GeV²
Data of Ref.(11)
normalised to Ref.(12)
dσ/dt (mb/GeV²)
-t (GeV²)
67687

Fig.3

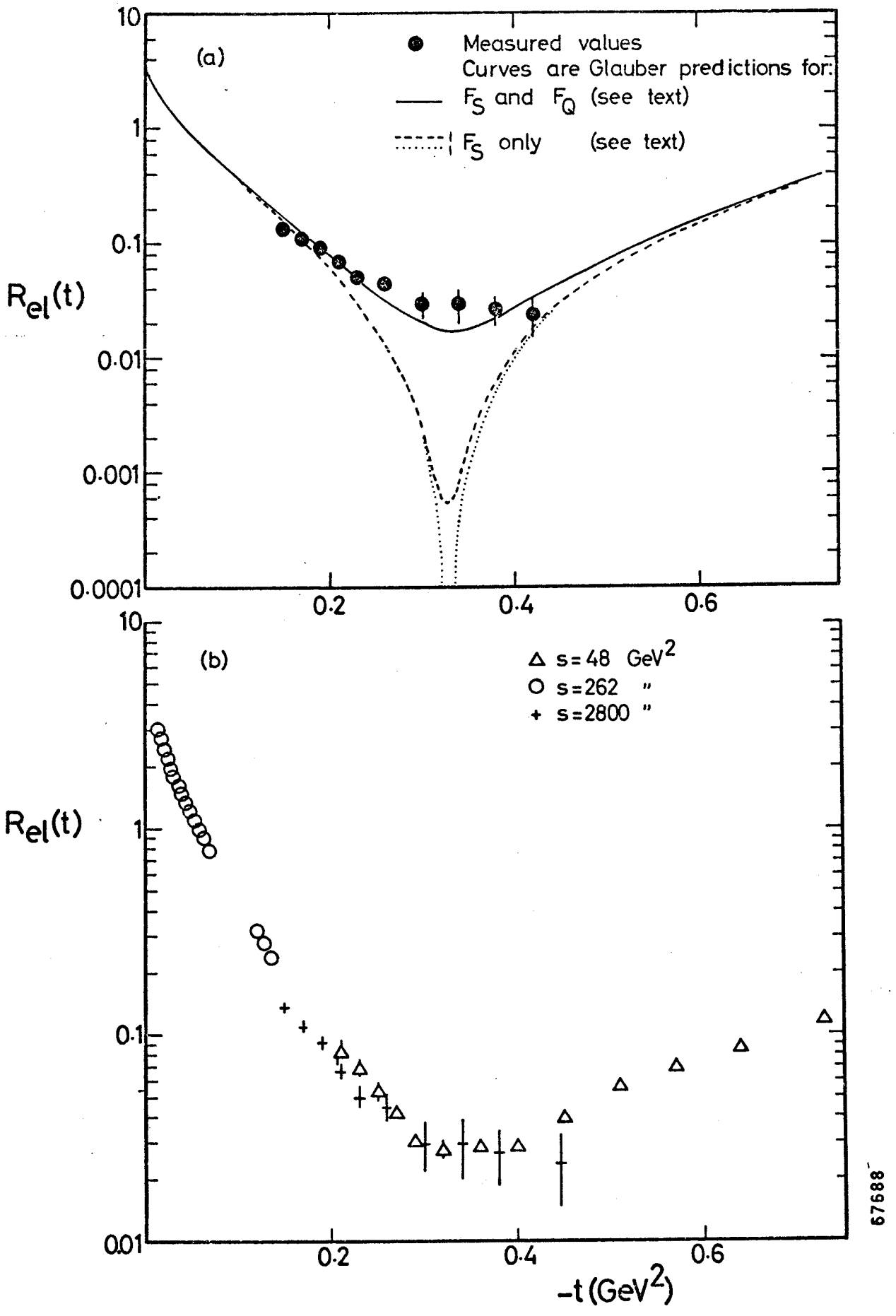
(a)
Measured values
Curves are Glauber predictions for:
F_S and F_Q (see text)
F_S only (see text)
$R_{el}(t)$
10
1
0.1
0.01
0.001
0.0001
0.2
0.4
0.6
(b)
Δ s=48 GeV^2
O s=262 "
+ s=2800 "
$R_{el}(t)$
10
1
0.1
0.01
0.2
0.4
0.6
$-t$ (GeV^2)
67688

Fig.4

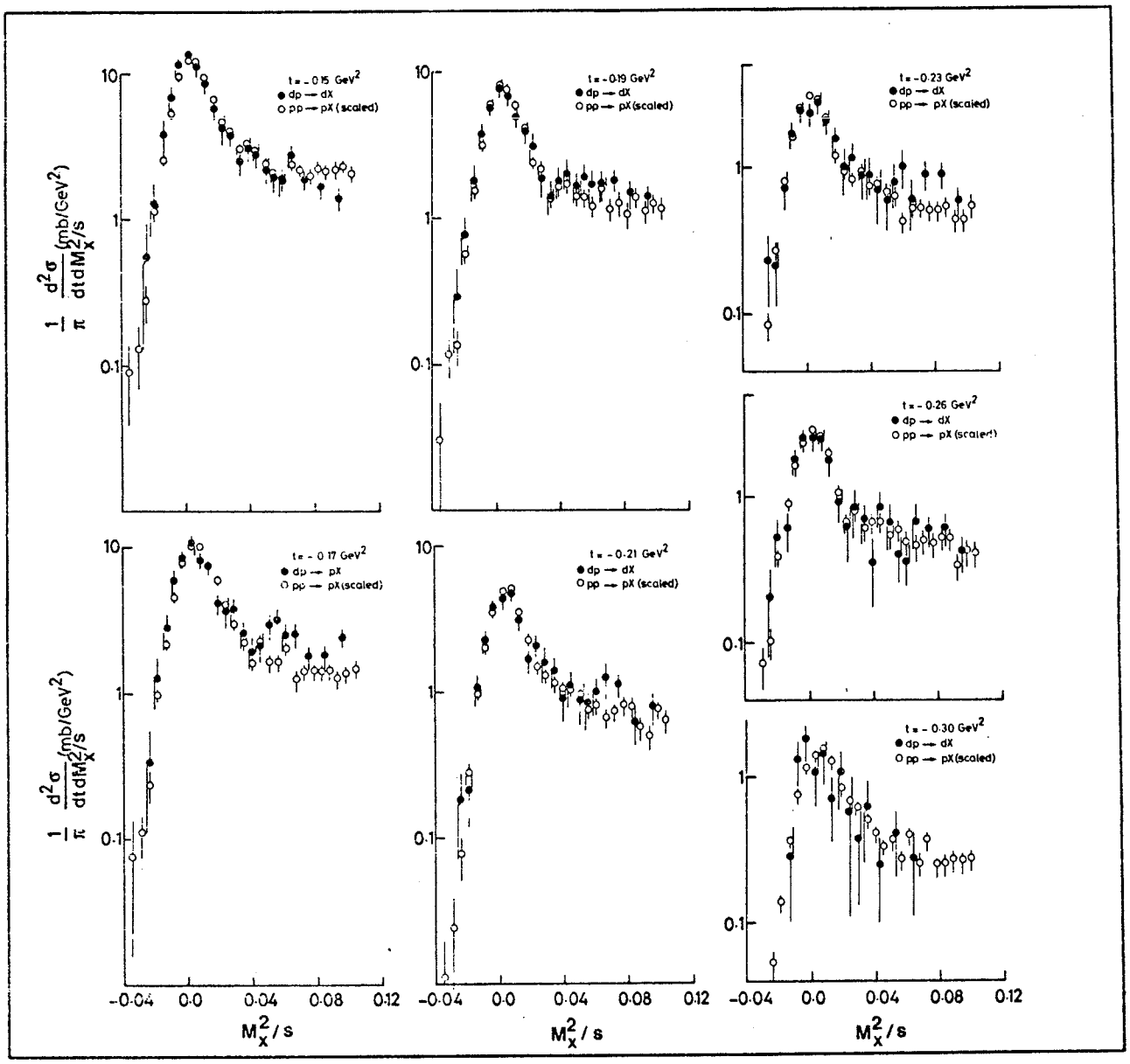
t = - 0.15 GeV²
t = - 0.19 GeV²
t = - 0.23 GeV²
t = - 0.17 GeV²
t = - 0.21 GeV²
t = - 0.26 GeV²
t = - 0.30 GeV²
● dp → dX
○ pp → pX (scaled)
$\frac{1}{\pi}\frac{d^2\sigma}{dt\,dM_X^2}$ (mb/GeV²)
M_X^2/s
-0·04
0·0
0·04
0·08
0·12
10
1
0·1
67259

Fig.5

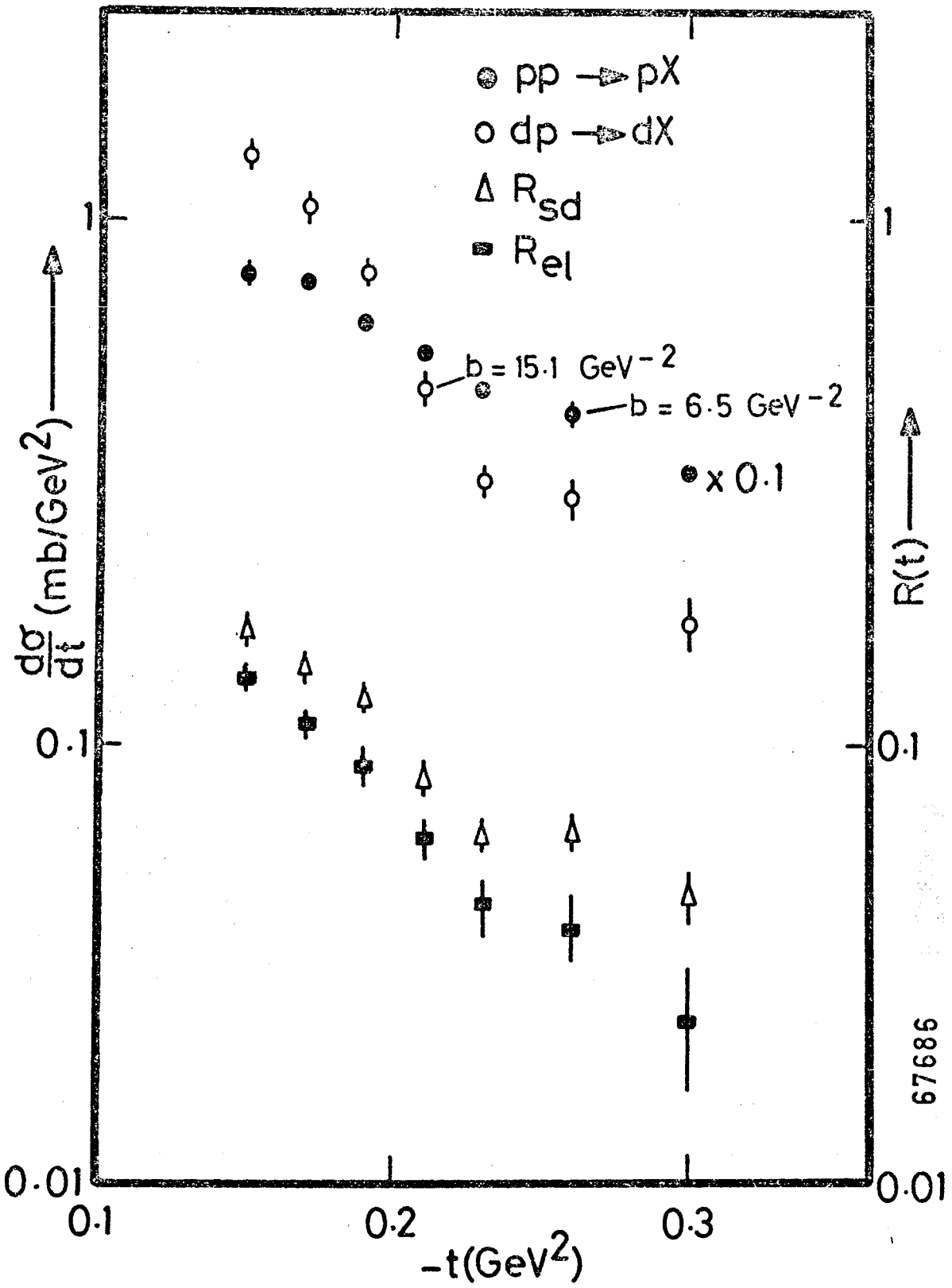
pp → pX
dp → dX
R_{sd}
R_{el}
b = 15.1 GeV^{-2}
b = 6.5 GeV^{-2}
x 0.1
$\frac{d\sigma}{dt}$ (mb/GeV^2)
R(t)
1
0.1
0.01
0.1
0.2
0.3
$-t(GeV^2)$
67686

Fig.6